Sustainable Energy & Fuels

ROYAL SOCIETY OF CHEMISTRY

PAPER

View Article Online
View Journal | View Issue

Cite this: *Sustainable Energy Fuels*, 2024, **8**, 5856

Structure–reactivity relationships governing hydrothermal liquefaction of lignin from co-solvent enhanced lignocellulosic fractionation (CELF)†

Heather O. LeClerc, [a] Ronish M. Shrestha,[a] Feng Cheng,[a] Alex R. Maag, [a] Geoffrey A. Tompsett,[a] Brent Scheidemantle,[b] Zhaoxi Zheng,[c] Klaus Schmidt-Rohr, [c] Amy M. McKenna, [de] Sydney Niles,[d] Jialiang Zhang,[f] Marcus Foston, [f] Charles M. Cai, [b] Andrew R. Teixeira [a] and Michael T. Timko *[a]

This study advances the fundamental understanding of the correlation between lignin structure and reactivity during hydrothermal liquefaction (HTL). Five different lignin varieties were obtained using the cosolvent enhanced lignin fraction (CELF) pretreatment; lignin sources were selected to represent a range of lignin types including softwood (pine), hardwood (poplar and maple), and agricultural (bagasse and corn stover) feeds and analyzed using conventional methods and new developed advanced solid-state ^{13}C NMR (ssNMR) approaches. Molecular weight, relative quantities of syringol (S), guaiacol (G), and *p*-hydroxyphenyl monomers, as well as degree of condensation (DC) were measured for the lignin samples, providing a quantitative basis for structure–reactivity relationships. These lignin samples then underwent HTL at 300 °C for 1 h, and the resulting biocrude, water soluble, char, and gas products were quantified. Lignin properties were correlated to HTL yields and biocrude composition, which found feedstock S/G ratio as the strongest predictor of biocrude and char yields, followed closely by DC. Ultrahigh resolution mass spectrometry analysis of the biocrude was used to gain mechanistic insights into lignin reactivity during HTL, finding that biocrude consists of oligomers of lignin subunits composed of 2–5 monomers. The biocrude obtained from high S content lignin is enriched in dimers and trimers, explaining the high biocrude yields obtained from these feeds compared with low S content lignin. These insights significantly advance current understanding of lignin reactivity under hydrothermal conditions.

Received 19th September 2024
Accepted 30th October 2024

DOI: 10.1039/d4se01294a

rsc.li/sustainable-energy

Introduction

Lignin is a major component of lignocellulosic biomass that is a byproduct of paper production as well as many of the proposed methods for converting cellulosic feedstocks into fuels.[1–4] Currently, no commercial technology exists for transforming lignin to high-value products besides lignin combustion for heat generation or the production of lignosulfonates.[5–7] Despite this, lignin's unique chemical moieties suggest the potential to serve as an abundant, renewable building block for aromatic fuels and chemicals due to its constituent aromatic monomers, abundance, and high carbon content.[1,3] Lignin is the most abundant natural source of aromatic molecules, and therefore its valorization demands further ressearch.[8]

Structurally, lignin is a highly complex, amorphous, and irregular material,[9,10] and incomplete lignin characterization hinders progress towards its valorization as a chemical or fuel precursor.[11] Lignin is composed of three primary building blocks: *p*-coniferyl alcohol, sinapyl alcohol, and *p*-coumaryl alcohol.[10] These building blocks are formed through the phenylpropanoid pathway in plants, starting from the well-known guaiacol (G), syringol (S), and *p*-hydroxyphenol (H) structures.[10] Different plant and wood types contain differing amounts of G, S, and H units. Lignin in softwoods, such as pine, is composed nearly exclusively of variously linked G-units, whereas hardwood lignin consists of both G- and S-units.[10] All three monolignols are typically found in agricultural biomass, such as that from sugarcane waste byproducts.[10] Besides the complexity of the monomers themselves, lignin is the polymeric result of radical and cross-coupling reactions,[11] resulting in

[a]*Department of Chemical Engineering, Worcester Polytechnic Institute, 100 Institute Rd, Worcester, MA 01609, USA. E-mail: mttimko@wpi.edu*

[b]*Bourns College of Engineering-Center for Environmental Research and Technology (CE-CERT), University of California, Riverside, CA 92507, USA*

[c]*Department of Chemistry, Brandeis University, 415 South Street, Waltham, MA 02453, USA*

[d]*National High Magnetic Field Laboratory, 1800 Paul Dirac Dr., Tallahassee, FL 32310, USA*

[e]*Department of Soil & Crop Sciences, Colorado State University, Fort Collins, Colorado 80523-1170, USA*

[f]*Department of Energy, Environmental, and Chemical Engineering, Washington University in St. Louis, 1 Brookings Drive, St. Louis, MO 63130-4899, USA*

† Electronic supplementary information (ESI) available. See DOI: https://doi.org/10.1039/d4se01294a

monomer–monomer linkages consisting of various types of C–O bonds, as well as C–C bonds between G-units.[10]

Traditional methods of lignin utilization involve co-processing of lignin with other biomass components, including gasification, pyrolysis, hydrothermal processes, and biological deconstruction.[8] Gasification produces low-value products such as heat and gaseous hydrocarbons,[12] whereas pyrolysis thermally reacts dry feeds to produce an unstable liquid bio-oil, which requires extensive upgrading to become a useful product.[13] Hydrothermal liquefaction (HTL) and the kindred method of solvothermal liquefaction (STL) are emerging technologies for converting high-moisture feeds into a useable biocrude oil,[14] capable of achieving positive energy balances for processing of the wet lignin feeds resulting from pulp and paper manufacturing. HTL of lignin produces a biocrude that can be upgraded to an aromatic-rich fuel additive or chemical feedstock.[15] From simple structural analysis, significant reactivity differences are expected between syringol, which bears two methoxy groups and a hydroxy group, compared with guaiacol, which bears a single methoxy group in addition to a phenol group.

Although the relationship between lignin structure and reactivity in a thermochemical environment such as pyrolysis or HTL is not well understood, some general trends have emerged from the kindred field of lignin extraction. Typically, lignin with high S-content has abundant labile β-*O*-4′ linkages, and high density of these bonds may serve to increase depolymerization efficiency.[16–18] For example, Santos *et al.*[19] found a linear correlation between lignin S/G ratio and bulk delignification rate constant in both saw dust and wood chips, indicating that syringyl units play a key role in lignin reactivity during the Kraft process. Additionally, due to the C–C bonds linking many G-units, the S/G ratio is inversely correlated with lignin condensation during extraction,[18] meaning that in S-rich lignin there are potentially fewer C–C bonds to break, which facilitates subsequent lignin depolymerization.

In addition to monomer type, other structural properties can impact lignin reactivity. For example, Nakagame *et al.*[20] showed that increasing pretreatment severity condensed the lignin structure, thereby decreasing lignin reactivity. Degree of condensation (DC) serves to quantify the average number of C–C linkages of a monomer, wherein a sample with a high degree of condensation is highly cross-linked with many monomer–monomer connections.[21] Similarly, molecular weight is an important factor impacting HTL reactivity of lignin, since a lower molecular weight lignin requires less depolymerization to form biocrude than a higher molecular weight version consisting of the same monomers and linkage types. HTL of lignin produces four primary product phases: water soluble organics (aqueous), biocrude, solid (char), and gas. To a first approximation, the difference between aqueous phase products, biocrude, and char corresponds to differences in molecular weight and inherent hydrophobicity of functional groups.[22,23] Accordingly, HTL of a higher molecular weight lignin might reasonably result in increased char and biocrude yields than reaction of a lower molecular weight lignin bearing the same monomer distribution, which would tend to form water-soluble products more readily.[23] Therefore, molecular weight and HTL yields would be expected to exhibit a positive correlation, especially if depolymerization during HTL was incomplete. To date, this remains an untested hypothesis.

While previous studies have focused on lignin isolated through the Kraft process, co-solvent enhanced lignocellulose fractionation (CELF) has emerged as a mild pretreatment method that enables extraction of low molecular weight and highly pure lignin.[24–26] CELF has potential for reliable production of lignin with consistent properties, and the use of CELF lignin in HTL valorization studies can help reduce uncertainty arising from residual cellulose content or sulfur in lignin obtained using other processes, including Kraft lignin.[27–29] CELF is a one-pot pretreatment process that uniquely employs renewable tetrahydrofuran (THF) as a monophasic co-solvent with water to accelerate the dilute acid solvation and extraction of lignin from biomass while simultaneously enhancing the deconstruction of the remaining sugar fractions.[24,30] The role of acid in the CELF process is to catalyze aqueous phase hydrolysis and dehydration, reactions that are responsible for the breaking of aryl-ether and glycosidic bonds. Isolation of CELF lignin by precipitation after boiling off and recovering the highly volatile THF provides a low-cost method for producing high quality lignin intermediates for further valorization[31–33] without influencing the separate processing of biomass sugars, conducive to lignin-first biorefining approaches.[28] Unlike lignin produced during paper making, CELF lignin is low in sulfur and can be considered "pure lignin". Relative to the organosolv method, CELF uses a superior lignin solvent and less acid to recover lignin at much higher efficiency.

Improved understanding of structure–reactivity relationships of lignin is crucially needed for advancing HTL and related lignin valorization methods. In this study, lignin from five different biomass feedstock types was extracted by CELF[24–26] pretreatment and then subjected to hydrothermal processing (at 300 °C for 1 h). The lignin samples were analyzed using a combination of standard techniques and newly developed advanced solid-state ^{13}C-NMR (ssNMR) approaches to quantify molecular weight, relative proportions of key monomers (syringol-to-guaiacol ratio, S/G), and degree of condensation (DC). The new ssNMR analyses are specifically tuned to characterization of CELF lignin, as it is structurally distinct from other types of lignin. After HTL processing, the resulting carbon yields of the biocrude, char, gas, and aqueous phases were quantified and in-depth compositional analysis of the biocrude phase was performed. Correlation coefficient analysis was applied to link lignin structure with product yields and biocrude properties. Biocrude was further analyzed *via* 21 tesla Fourier-transform ion cyclotron resonance mass spectrometry (21T FT-ICR MS) to gain insight into the presence of dimers, trimers, and other oligomers that can be used to understand the response of biocrude to hydrotreating. These results provide new insight into the role of monomer content and degree of condensation on lignin reactivity under HTL conditions.

Materials and methods

Biomass materials

Five types of biomass were used as feedstocks in this study: sugarcane bagasse, poplar wood, pine wood, corn stover, and maple wood. Lignin was isolated from the biomass using the CELF process at UC Riverside. Kraft lignin (Sigma-Aldrich) derived from spruce wood was used as a standard for comparison to CELF lignin. Acetone (purity > 99.5%, Sigma-Aldrich) was used as the solvent for biocrude recovery and reactor cleaning. All lignin samples were dried in an oven at 65 °C overnight to obtain accurate, moisture-free weights for reactor loading. Deionized water (electrical resistivity >18.0 MΩ cm) was used for HTL reactions. Helium gas (grade 5.0, Airgas) was used to purge and pressurize the HTL batch reactor prior to each run and also as the carrier gas for gas chromatography.

CELF pretreatment

CELF pretreatment was conducted at the University of California Riverside as described in other studies.[33] Biomass was first milled and screened to 2 mm particle size before loading into a 1 L Hastelloy Parr autoclave reactor (236HC series, Parr Instruments Co., Moline, IL, USA) equipped with twin pitched-blade Rushton impellers. Reactor loading was chosen to maintain a solid content of 7.5 wt% in a 1 : 1 (w/w) THF–water solution and dilute sulfuric acid (0.05 M). CELF took place at 150 °C and 25 min for agricultural feedstocks, and 160 °C and 15 min for soft- and hardwood feedstocks, as determined to be optimal for maximizing lignin extraction while minimizing lignin condensation and minimizing sugar loss.[25,34,35] Additional experiments were performed on poplar lignin to confirm selection of CELF extraction conditions appropriate for production of lignin to be used during HTL experiments, as shown in Fig. SI-8.† All reactions were maintained within ±1 °C by convective heating using a 4 kW fluidized sand bath (Model SBL-2D, Techne, Princeton, NJ, USA). Temperatures were monitored using an internally fixed thermocouple (Omega, K-type) before reaction quenching took place in a large room-temperature water bath at the end of the allotted reaction time. The resulting cellulose-rich solids were separated from the pretreatment liquor containing lignin *via* vacuum filtration through filter paper.

The collected liquid fraction was titrated to pH 6.5–7 using ammonium hydroxide and then transferred to a rotary evaporator to boil off the THF (60 °C, −0.75 MPa, 2–3 h). Precipitated lignin was then dried overnight in a 50 °C oven. The dry lignin was then pulverized by mortar and pestle and washed with diethyl ether and water to remove residual soluble impurities before being dried again in the oven overnight to a moisture content of less than 5%. CELF lignin recovery varied from 78% (for corn stover) to 85% (for poplar and maple), as determined gravimetrically. Lignin samples obtained from the CELF pretreatment are named by their source with "C" prefix, *e.g.*, C-Poplar.

Hydrothermal liquefaction of lignin

HTL reactions were conducted in a 300 mL stainless-steel bench-top reactor (Model 4841, Parr Instrument Co., Moline, IL, USA) equipped with a magnetic stirring drive. The lignin slurry (100 g, 10 wt% solids) was loaded into the reactor, sealed, and the reactor was weighed, purged with nitrogen to remove residual oxygen, pressurized with nitrogen to 7.6 MPa, and heated to 300 °C (~6 °C min^{-1}) using a heating jacket. HTL conditions were selected after preliminary experiments revealed that biocrude yields are weakly dependent on reaction temperature over the range from 300 to 350 °C, as shown in Fig. SI-8.† At reaction temperature, the pressure was 20.7 ± 0.3 MPa, sufficient to maintain >92.3% of the water fed to the batch reactor in its liquid state. Reaction temperature was maintained within ±2 °C for 1 h, at which point the reaction was quenched by placing the reactor in a water-ice bath. All HTL runs were performed in at least duplicate with the measured product yields consistent to within ±5%. Average values are reported here along with uncertainties estimated from repeated tests.

After quenching and depressurization, gas yield was determined by gravimetric difference before and after reaction. The reactor contents were poured into a vacuum filter to separate the aqueous phase from the biocrude–char mixture. The isolated biocrude and char mixture was then rinsed with acetone to separate the biocrude from the char phase and the extract was placed in a rotary evaporator to remove residual acetone. The bottom-up carbon mass balance, determined as the sum of the gravimetric yields of oil, gas, aqueous, and char combined with their fractional carbon content, always closed to within 5%, similar to recent reports on HTL mass balance closure.[22,36] Losses are due to the limited precision of the top loading analytical balance used to estimate gas yield by difference (±1.0 g out of 16 000 g) and residual material in the reactor fittings, pressure transducer, *etc.* Of these, underestimation of gas yields will account for >50% of the mass balance closure gap, given the precision of the analytical balance used for reactor weight measurements. Given the small gas yield relative to other products, uncertainty in the gas yield has a negligible effect on any conclusion made here.

Solid-state ^{13}C NMR of lignin

Solid-state nuclear magnetic resonance spectroscopy (ssNMR) was performed using a Bruker Neo Avance 400 spectrometer at a ^{13}C NMR frequency of 100 MHz. The instrument utilized a Bruker double-resonance magic-angle spinning probe head for 4 mm rotors. Samples filled the 9 mm long radio-frequency coil from end to end where a cylindrical glass plug of 3 mm height at the bottom of the rotor prevented sample material from being placed outside the coil. A 14 kHz spinning frequency was used for all samples unless otherwise stated. Direct polarization (DP) with a recycle delay of 20 seconds was used for the corn stover sample, which showed short spin–lattice relaxation times, presumably due to unpaired electrons. For most other samples, multiple cross polarization (multiCP)[37] was employed with 6 repolarization delays. Recoupled dipolar dephasing[37] before detection was used to obtain selective spectra of C not bonded to H and mobile segments such as rotating CH_3 groups. Additional information and equations for composition quantification can be found in the ESI.†

Gel permeation chromatography (GPC) of lignin

GPC analysis was performed in a Waters e2695 system with a 2489 UV detector (256 nm) on a three-column sequence of Waters™ Styragel columns (HR0.5, HR1, and HR3). Tetrahydrofuran (THF) was used as eluent, and the flow rate was 1.0 mL min^{-1} 10 mg sample was then dissolved in 1 mL of THF and filtered through a 0.22 μm nylon membrane filter with an injection volume of 50 μL. Molecular weights (M_n and M_w) were calibrated against a polystyrene calibration curve. A calibration curve was constructed by fitting a third-order polynomial equation to the retention volumes obtained from six narrow polystyrene standards and two small molecules (diphenylmethane and toluene) ranging in molecular weight from 92 to 3.4×10^4 g mol^{-1}. The curve fit had an R^2 value of 0.99.

Elemental analysis & total organic carbon of HTL products

Elemental analysis of all lignin, biocrude, and char samples was performed at Midwest Microlabs (Indianapolis, IN, USA) to obtain carbon, hydrogen, nitrogen, and sulfur content. Oxygen content was determined by difference. The carbon content of the resultant aqueous phase was measured using a Shimadzu total organic carbon (TOC) analyzer. The carbon yields were determined using eqn (1), which utilizes the measured product mass and resultant carbon weight fraction of each phase and the initial feed.

$$\text{Carbon yield}_{\text{product}} = \frac{\text{mass}_{\text{product}} \times \text{carbon\%}_{\text{product}}}{\text{mass}_{\text{lignin}} \times \text{carbon\%}_{\text{lignin}}} \times 100 \quad (1)$$

Carbon yields in the product phases were summed to check for overall carbon balance closure, wherein all cases the carbon balance closed to within 5%.

Gas chromatography MS & FID of HTL biocrude

Biocrude composition was analyzed using a Shimadzu QP 2010 SE gas chromatography-mass spectrometry (GC-MS) system. The major monomers identified using MS were then quantified using flame ionization detection (FID), also from Shimadzu. For GC-MS, a SHRZI-5MS column (30 m × 0.25 mm ID × 0.5 μm thickness) was utilized whereas for GC-FID the column was an Rt-Q-BOND (30 m × 0.25 mm ID × 85 μm thickness). Both analyses utilized the same temperature program consisting of an initial column temperature of 35 °C that increased at a rate of 3 °C min^{-1} to 290 °C, at which point the temperature was held for 5 minutes. The injector temperature was set to 300 °C with an injection volume of 3 μL.

21 Tesla Fourier transform ion cyclotron resonance mass spectrometry (FT-ICR MS) of HTL biocrude

A custom-built 21T FT-ICR MS[38,39] was used to analyze biocrude products utilizing positive-ion atmospheric pressure photoionization (+APPI). Samples were prepared by first dissolving them in a 50/50 (volume) mixture of toluene and tetrahydrofuran to a final concentration of 125 μg mL^{-1} prior to analysis. Further details on FT-ICR MS analysis can be found in previous reports and literature.[22,36,40]

Results & discussion

Lignin composition, purity, and processing effects

The goal of this work is to explore the relationship between lignin structure and reactivity under hydrothermal conditions. Understanding the relationship between lignin structure and reactivity requires a set of well characterized lignin substrates.[11,41–43] The CELF process was used as a feedstock-agnostic method of separating lignin from other biomass constituents. CELF entails treatment at temperatures and acid conditions that can modify lignin structure, including disruption, rearrangement, and formation of interunit linkages and potentially reduction of molecular weight,[29] meaning that detailed characterization of the CELF samples was required before they could be used as the basis for structure–activity relationships. Beginning with elemental composition, the carbon content of the five CELF lignin samples included in this study averaged 68 ± 3% and the oxygen content averaged 25 ± 3% (Table SI-1†). Compared with a traditional Kraft lignin (K-Spruce) used as a benchmark, the CELF lignin samples consisted of more carbon (68 compared with 63 wt%) and less oxygen (25 compared with 31 wt%). K-Spruce contains 2.8 wt% sulfur, whereas the sulfur content of the CELF lignin samples varied from 0.89 to 2 wt%.

Due to the unique spectral and structural differences in CELF lignin compared to native or Kraft lignin detailed below, new solid-state ^{13}C NMR (ssNMR) methods were developed for quantitative characterization of CELF lignin. While solution NMR is more commonly used for lignin analysis than ssNMR,[29] solid-state ^{13}C NMR has distinct advantages over heteronuclear single quantum coherence (HSQC) solution-phase NMR, which uses proton detection and can therefore not directly analyze the substituted aromatic carbons abundant in lignin. As a result, ssNMR can be used for reliable determination of the C–C bonds crucial to DC, even for re-arranged lignin types such as CELF lignin, whereas HSQC cannot. In addition, ssNMR cannot be influenced by incomplete-solubility issues that may arise in solution-phase NMR. Further, ssNMR as performed here is nearly quantitative[37,44,45] and does not require derivatization, which can introduce uncertainty.[29,41,45,46]

Comparison of ssNMR spectra of CELF lignin samples (Fig. 1) and corresponding whole biomass (Fig. SI-1 and SI-2†) revealed that all lignin spectra exhibited strong aromatic signals between 165 and 100 ppm. In contrast, carbohydrate bands associated with cellulose and hemicellulose in the 110–60 ppm range dominated the biomass spectra. While the CELF lignin spectra still contained signals between 95 and 50 ppm, these were mostly attributed to OCH_3 aromatic lignin substituents (~56 ppm) and the three nonaromatic carbons in the repeating lignin subunits that are usually oxidized to sp^3-hybridized OCH and OCH_2 forms. Accordingly, ssNMR analysis confirms that most cellulose had been removed from CELF lignin, as indicated by the disappearance of signature cellulose peaks between 120 and 80 ppm following the CELF process.

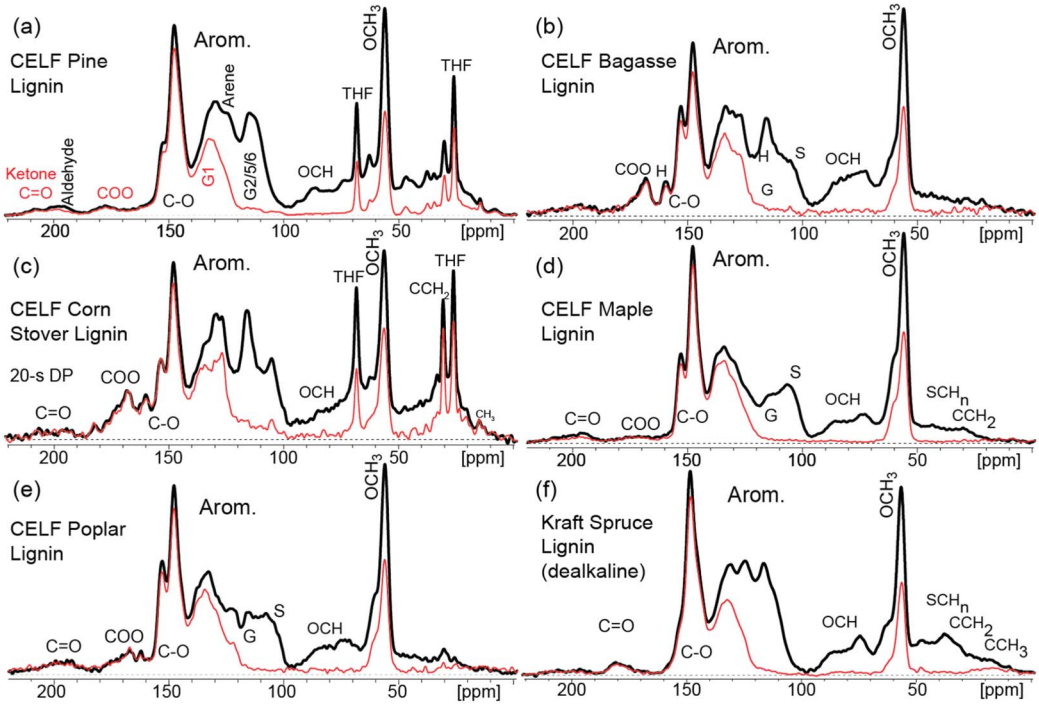

Fig. 1 Nearly quantitative solid-state multiCP ^{13}C NMR spectra of six lignin samples extracted from wood and agricultural biomass. Corresponding spectra after dipolar dephasing are also shown (thin red traces). Assignments of prominent peaks are given in the spectra. (a) Softwood C-Pine lignin (b) agricultural C-Bagasse lignin. (c) Agricultural C-Corn stover lignin. (d) C-Maple lignin, (e) C-Poplar lignin, and (f) representative Kraft softwood spruce (K-Spruce) lignin. S: syringol; G: guaiacol resonances. Reference lignin spectra can be found in Fig. SI-3.†

In addition to confirming the removal of cellulose and hemicellulose, NMR analysis revealed trace tetrahydrofuran (THF) peaks due to incomplete drying in CELF corn stover (C-Corn Stover) lignin and CELF Pine (C-Pine) lignin. Purchased Kraft hardwood lignin samples were found to contain unusual impurities at high levels certain to influence reactivity (Fig. SI-3†), CELF processing was confirmed to be a source of clean representative lignin suitable for reactivity analysis.

The finer structure of the aromatic bands in the ssNMR spectra provides information about monomer content. The peak area between 157 and 142 ppm corresponds mostly to aromatic C–O carbons within guaiacol and syringol rings. C-Pine and K-Spruce lignin spectra lacked the peak around 152 ppm present in the remaining samples, which is assigned to the OCH_3-substituted S3 and S5 carbons in etherified syringol units, consistent with its absence in these syringol-free softwood samples.[47] Compared to spectra of all C (black traces), dipolar dephasing (red traces) (Fig. 1) provides selective spectra of C not bonded to H or CH_3 groups; this convenient spectral editing by gated decoupling[37,48] is unique to solid-state NMR. Specifically, within the core aromatic region (141–110 ppm), all dipolar dephased spectra contained a major peak near 135 ppm from the S1 and S4 carbons in syringol and G1 in a guaiacol ring, as well as G5 if carbon-substituted. An additional peak near 127 ppm attributed to C1 of *p*-hydroxyphenyl rings was present in C-Bagasse and C-Corn Stover lignin, consistent with their classification as agricultural samples. The peak at 56 ppm (OCH_3) was found to decrease to ~57% of its full intensity after dipolar dephasing, as is typical for the spin dynamics of a rotating methyl group located in a rigid environment[37] and directly verified in clean hardwood lignin by comparison with the unselective spectrum.

Comparing the dipolar-dephased ^{13}C NMR spectra of the CELF lignin samples with their corresponding native-lignin spectra (Fig. 2) in the spectral region of 160–40 ppm provided information about structural changes resulting from lignin extraction and enabled determination of the S/G ratio and the degree of condensation. The intensity of the syringyl C–O peak at 152 ppm was decreased due to acid-catalyzed hydrolysis of syringyl ethers,[49] which makes the traditional determination of S/G ratio by deconvolution of the C–O line shape[50] impractical for CELF lignin. Instead, the intensity of the prominent OCH_3 signal at ~56 ppm, relative to the combined S + G aromatic C–O signal between 157 and 142 ppm, was used to determine the ratio of syringol (two OCH_3 groups) to guaiacol (one OCH_3 group), specifically as a lower limit due to the potential for hydrolytic OCH_3 loss. The shoulder near 62 ppm was included with the OCH_3 intensity of lignin after it had been confirmed, using two-dimensional (2D) NMR, to behave exactly like the main OCH_3 peak (Fig. SI-4 and SI-5†). Details of this quantitative analysis are presented in the ESI.† For agricultural biomass, the deconvolution process through spectral editing also considered the =CH of ferulate and similar alkenes (Fig. SI-6†).

In addition, S/G ratio was determined by deconvolution of the full hardwood- or biomass-lignin spectra, using the spectrum of pine as a pure-G component, as shown in the ESI.† After

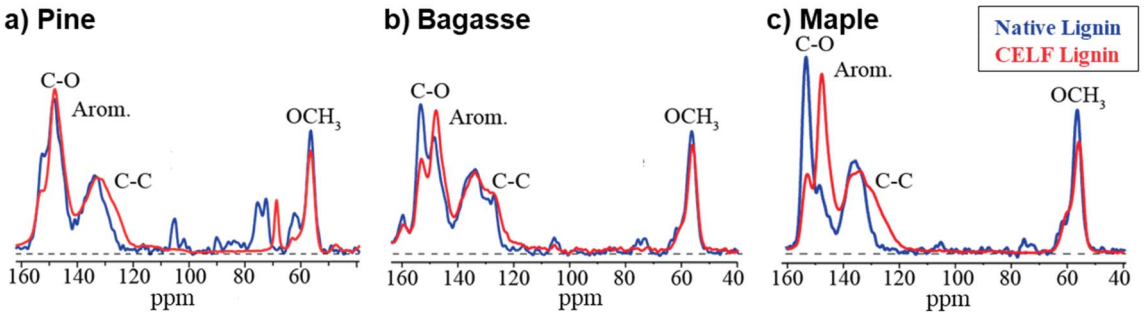

Fig. 2 Central regions of ^{13}C NMR spectra after dipolar dephasing of native lignin in wood or agricultural biomass (blue trace) and the corresponding extracted CELF lignin spectra (red trace) for a representative hardwood, softwood, and agricultural sample. (a) Pine, (b) sugarcane bagasse, and (c) maple.

subtraction of the G component matched near 120 ppm (Fig. SI-7†), the difference spectra show the characteristics of pure syringyl lignin, for instance with the distinctive peak of S2/5 resolved around 106 ppm. The fractions of the aromatic C–O integrals in this deconvolution are the G and S fractions.

Beyond monomer content, lignin decomposition behavior varies based on inter-unit bonding of the monomers to one another.[51] Identifying and quantifying all bond types using ssNMR is beyond the scope of this study. Nevertheless, the signal between 141 and 110 ppm, including additional intensity at 125 ppm attributed to C–C bond formation, can be analyzed to estimate the degree of condensation, *i.e.*, the fraction, per aromatic ring, of C–C bonds not involving C1. It contains signals from two carbons (S4 and S1) in syringol and from one carbon (G1) in a simple guaiacol ring without G5 substitution. This is the same as the number of OCH_3 carbons associated with these rings, so the excess of this signal near 135 ppm over the dephasing-corrected methoxyl signal is due to condensation, *i.e.* additional bonds of aromatic C with other carbons, beyond the standard bond at C1 of the lignol ring. The contribution from C1 of H-units at 127 ppm was also taken into account (see the ESI† for details of this analysis).

Using these new methods, the lignin S/G as well as the degree of condensation (DC) for CELF lignin samples and six similar reference lignin samples were estimated and compared (Table 1). HSQC NMR, being based on proton detection, cannot be used to analyze the nonprotonated carbons involved in the C–C bonds between guaiacol rings that are crucial for lignin condensation. Therefore, HSQC cannot reliably determine the degree of lignin condensation (DC) of the samples in this study. As expected, C-Pine (softwood) resulted in the lowest S/G (0.01) whereas the hardwood C-Maple and C-Poplar lignin samples were found to have the highest S/G of 0.85.

A comparison of lignin composition measured for CELF samples and reference samples obtained by enzymatic hydrolysis compiled in Table 1 provided insight into the chemical processes that accompany CELF. The most notable difference in S/G between the CELF and reference lignin samples was the significant decrease in hardwood S/G seen in both C-Maple and C-Poplar; native maple and poplar lignin extracted *via* enzymatic hydrolysis both exhibited S/G ratios greater than 1.0, consistent with literature on hardwood lignin composition,[18,52–54] while the CELF hardwoods both resulted in S/G lower than 0.9 (Table 1). As expected, the $S/G_{(d)}$ (*i.e.*, deconvoluted) ratios of the two agricultural samples, sugarcane bagasse and corn stover, are intermediate to the values measured for soft- and hardwood lignins. Literature shows sugarcane lignocellulose to have typical S/G ratios between 0.8 and up to 1.90, depending on their genotype,[55,56] whereas corn stover has been shown to have variable S/G due to dependence on extraction severity.[57] With increasing

Table 1 Wood type, sample name, and chemical structural characteristics of CELF and comparison lignin samples from ^{13}C NMR and GPC. Degree of condensation (DC) and syringol:guaiacol ratio (S/G) were calculated as described in the ESI

Wood type	Sample	DC	S/G	S/G_d (deconv.)	M_n	M_w
Softwood	C-Pine lignin	0.89	≥0.01	0.01	1185	2176
Agricultural	C-Bagasse lignin	0.58	≥0.33	0.70 ± 0.3	1125	1659
Agricultural	C-Corn Stover lignin	1.00	≥0.15	0.60 ± 0.3	1094	1598
Hardwood	C-Poplar lignin	0.47	≥0.63	0.85 ± 0.2	1082	1688
Hardwood	C-Maple lignin	0.57	≥0.67	0.85 ± 0.2	1782	2522
Softwood	K-Spruce lignin	0.95	≥−0.08[a]	0.0	—	—
Softwood	Pine wood	0.45	0.0 ± 0.05	0.0	—	—
Softwood	Loblolly pine lignin	0.40	0.01 ± 0.05	0.0	—	—
Agricultural	Sugarcane bagasse	0.17	0.35 ± 0.1	N/D	—	—
Hardwood	Enzyme poplar lignin	0.10	1.3 ± 0.4	0.8 ± 0.3	—	—
Hardwood	Maple wood	0.01	1.4 ± 0.3	1.4 ± 0.25	—	—

[a] Negative value indicates demethylation (hydrolysis and OCH_3 release).

enzymatic hydrolysis severity, corn stover S/G increases from values <1.0 and can reach values much greater than 1.0 (*i.e.* at 190 °C).[57] Furthermore, *p*-hydroxyphenyl (H) was present in both the bagasse and corn stover lignin (see Table SI-1†), as is typical for grassy biomass,[58] and absent from both types of wood. From this analysis, it can be concluded that the CELF process produces lignin with lower S/G ratios than in the precursor biomass, potentially due to C–O–CH_3 aryl-ether cleavage despite the relatively mild thermal conditions used during the extraction process.

ssNMR was also used to determine the degree of lignin condensation (DC) (Table 1). C-Maple and C-Poplar possessed the lowest DC of the samples included in this study, which was consistent with reference lignin samples. C-Corn Stover exhibited the highest DC of 1.00, whereas analysis of native bagasse found significantly lower DC (0.17). Interestingly, nearly all CELF lignin samples resulted in higher DC than the corresponding reference lignin (associated with new signals near 125 ppm in Fig. 2), apparently due to C–C bond formation at the temperature (>150 °C) and acidic conditions used in the CELF process.[11,57]

In addition to ssNMR analysis, gel permeation chromatography (GPC) was utilized to estimate the molecular weights of the five CELF lignin samples (Table 1). All number average molecular weights (M_n) of CELF samples fell between 1050 and 1200 Da with the exception of C-Maple lignin (M_n = 1780 Da). The weight average molecular weight (M_w) followed a similar trend to M_n with the exception of C-Poplar, which has the lowest M_n but the third highest M_w. This indicates that C-Poplar contained a larger proportion of low molecular weight components compared with the other four samples. Neither M_w nor M_n followed any discernible pattern related to the lignin type (hardwood, softwood, or agricultural).

Lignin hydrothermal liquefaction analysis

The five characterized CELF lignin samples underwent HTL at standardized conditions of 300 °C for 1 h before quantification of corresponding biocrude, char, aqueous, and gas yields. Additional experiments were performed on poplar, which was treated at several different CELF conditions and under HTL at both 300 and 350 °C before finalizing treatment conditions used for all other samples. Fig. SI-8† summarizes the results of these additional experiments. Gravimetric yields were used along with elemental analysis (Table SI-2†) to estimate product carbon yields, with the finding that biocrude yield and char yield were roughly equal to one another and consistently greater than aqueous phase and gas yields (Fig. 3). Biocrude yields ranged from 44 to 63 wt%, with variability between samples much greater than experimental uncertainty. C-Pine resulted in the lowest biocrude yield, whereas C-Poplar produced the highest amount of biocrude of the five CELF lignin samples. Char yield followed an inverse relationship with biocrude yield, wherein C-Poplar had the lowest char yield (18%) and C-Pine the highest (50%). Aqueous and gas phase carbon yields remained relatively constant across lignin types, as aqueous yields averaged ~12 ± 5% and gas yields averaged 4 ± 2%.

Biocrude composition was analyzed using gas chromatography mass spectrometry (GC-MS) to provide additional insights on HTL reactivity (Fig. SI-9†). GC-MS peak areas were compared to GC-FID (flame ionization detector) calibration curves to quantify monomer yields within the resultant HTL biocrude (Fig. 4). Biocrude obtained from C-Pine contained negligible syringol monomers, as expected, given the low syringol content of softwoods[2,9] and low S/G ratio of C-Pine (0.01) measured using ssNMR (see Table 1). HTL monomer yields in biocrude were modest, <25 mg g^{-1} lignin, which is consistent with incomplete depolymerization and subsequent repolymerization of monomers to form larger biocrude or char-phase compounds.[59,60] Guaiacol yields for all five samples fell between 7.5 and 10 mg g^{-1}, irrespective of the lignin source. As expected based on lignin S/G, syringol was identified in both agricultural and hardwood biocrudes, whereas ethyl phenol was only identified in C-Bagasse and C-Corn Stover biocrudes due to the presence of *p*-hydroxyphenyl units in the lignin feeds. Based on total monomer yield, agricultural feedstocks showed the greatest capacity for lignin monomer production from HTL due to the presence of hydroxyphenyl monomers. Further details, including estimated biocrude S/G ratios, are provided in Table SI-2.†

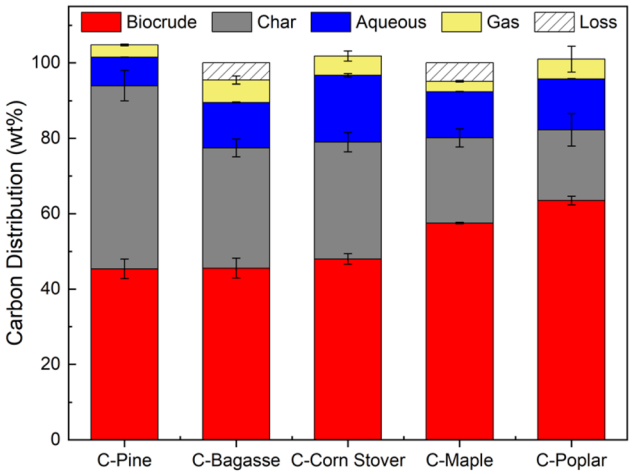

Fig. 3 Hydrothermal liquefaction product yields displayed in terms of carbon in the feed for each of the five CELF (C-) lignin samples. All experiments were conducted in at least duplicate, and averages and error bars are shown for each sample. All reactions were completed at 300 °C and 60 min reaction time.

The next step was to relate lignin structure to HTL reactivity. Accordingly, correlation coefficient analysis was performed on various combinations of lignin properties (inputs) and HTL product properties (outputs) (Fig. 5). Starting with biocrude yield and composition, correlation analysis revealed that biocrude yield was positively correlated with S/G ratio of the lignin feed and equally negatively correlated with lignin DC. Lignin molecular weight and elemental composition were found to play minor, secondary roles in determining biocrude yield. Biocrude monomer content, as indicated by the S/G ratio calculated from GC data, was strongly positively correlated with lignin S/G and secondarily negatively correlated with DC. For the samples included in this study, S/G and DC were inversely correlated with one another as a consequence of differences in S

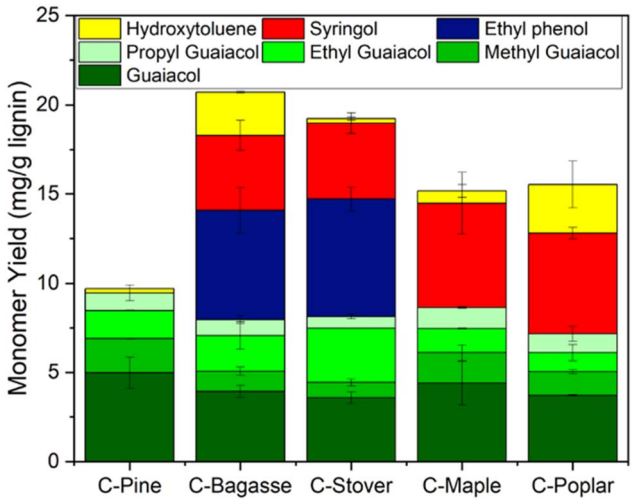

Fig. 4 Resultant monomer yields from hydrothermal liquefaction of CELF lignin in the biocrude phase. Monomers were identified *via* GC-MS and quantified using a calibration curve on GC-FID.

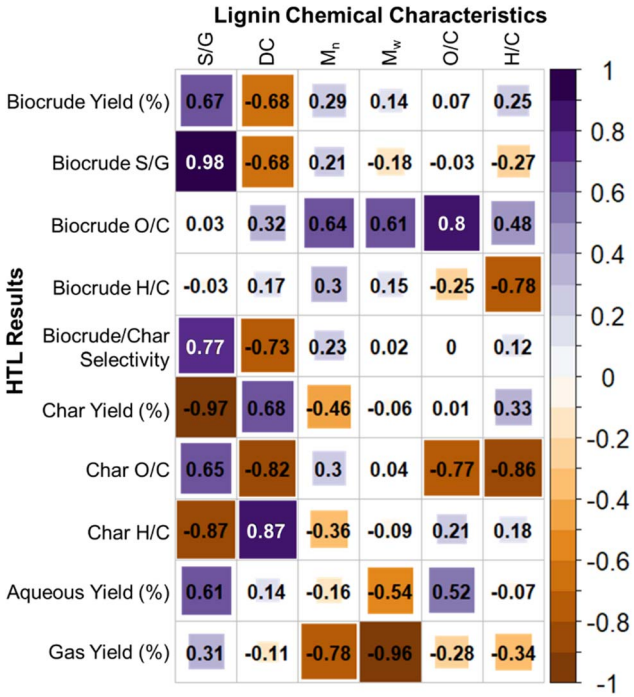

Fig. 5 Linear correlation coefficient matrix relating the impact of various lignin chemical structure characteristics on resultant HTL parameters. A value near +1 indicates a strong positive correlation, a value near −1 is a strong negative correlation and values close to 0 indicate no correlation.

and G structure, meaning the negative correlation between lignin DC and biocrude S/G content may be incidental and arise from differences in connectivity of the monomers. Biocrude monomer composition (S/G) was most strongly related to lignin monomer composition (S/G) and secondarily molecular weight.

Considering the remaining HTL product phases, char yield was found to have a strong negative correlation with lignin S/G and positive correlation with lignin DC, mirroring the correlations observed for biocrude yield. Interestingly, char yield was negatively correlated with M_n, indicating that increased lignin polymer size results in decreased char for these samples. Char O/C was strongly dependent on the feed composition, whereas char H/C was mainly dependent on lignin structure (*i.e.* S/G ratio and DC). Aqueous yields were moderately correlated with several factors, namely lignin S/G, O/C, and M_n. Despite gas yields showing strong inverse correlations with M_n and M_w, these yields were too low (<5% carbon) for meaningful interpretation.

Since biocrude yield is an important factor in determining economic feasibility of an HTL process,[22] the observed correlations have two significant implications: (1) technologically, high S/G ratio lignin is the preferred feed for HTL processes, (2) scientifically, the low correlation between lignin polymer size and biocrude yields indicates that lignin depolymerization must proceed to the point that the oligomers achieve biocrude and aqueous phase solubility in terms of size, structure, and composition, before partially repolymerizing to form heavier biocrude and eventually char. The strong positive correlation between lignin S/G ratio and biocrude yield is consistent with the assertion made in the literature without experimental substantiation, that lignin conversion to small molecules is determined largely by monomer reactivity and hence propensity to repolymerize.[18,19,53]

Analysis of the heavy fraction of biocrude

GC-MS analysis revealed that monomer yields were always <20 mg g^{-1}, indicating the majority of biocrude must be composed of compounds other than monomers and that are insufficiently volatile to be vaporized at 300 °C. The composition of the nonvolatile fraction of the biocrude provides further clues into reactivity; moreover, knowledge of the composition of the nonvolatile fraction is required for hydrotreating of the biocrude to produce fuels, fuel additives, and chemical feedstocks.[61–63] Accordingly, HTL biocrude was analyzed using Fourier transform ion cyclotron resonance mass spectrometry (FT-ICR MS) to understand the molecular compositions associated with biocrude, especially for components that could not be analyzed using GC due to low volatility.

FT-ICR MS coupled to atmospheric pressure photoionization (APPI) provides precise molecular formulas based on ppb-level m/z resolution that can be used to determine the number of carbons, hydrogens, heteroatoms, and double bond equivalents (*i.e.*, double bonds or rings). Fig. 6 is a plot of the number of oxygen atoms contained in a particular compound as a function of the number of carbon atoms in the same compound. Plotting oxygen atom content as a function of carbon atom content results in a distinct, near-linear trend for both the C-Maple and C-Bagasse biocrudes. The linear relationship between oxygen atom and carbon atom content is consistent with the trend expected for oligomers composed of lignin subunits, such as guaiacol and syringol. For both C-Maple and C-Bagasse, oxygen and carbon are present roughly in a 1 to 5 ratio, indicating that for an increase in oxygen number by one, carbon number

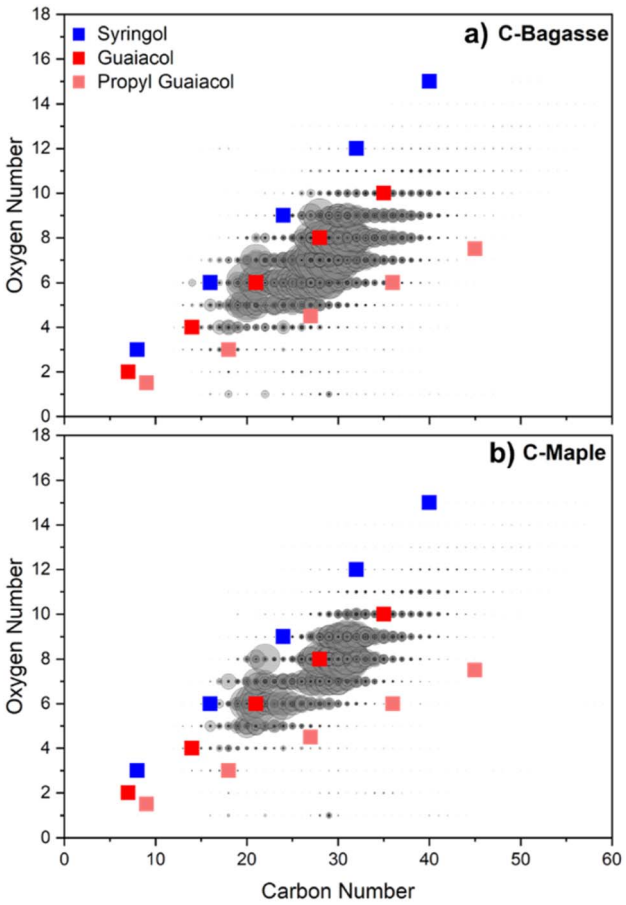

Fig. 6 Relationship between oxygen number and carbon number of the compounds identified in HTL biocrude by (+) APPI 21 tesla FT-ICR MS for (a) C-Bagasse biocrude and (b) C-Maple biocrude. Data points are sized by relative abundance. Red and blue markers represent theoretical guaiacol and syringol oligomers, respectively.

increased by around 5, somewhat less than would be expected for an oligomer consisting entirely of S units and consistent with the ratio expected for a mixture of lignin subunits.

Fig. 6 offers an opportunity to identify specific compounds in the biocrude. To this end, the FT-ICR MS data were carefully analyzed for the presence of specific compounds, for example a syringol or guaiacol dimer or trimer. Unfortunately, the spectra are too complex for such simple analysis; as an example, the biocrude obtained from C-Bagasse consists of 12 250 distinct formulas, excluding isomers. Instead, basic polymerization trends for three lignin monomeric units, corresponding to the expected O/C ratio of syringol (2.5 oxygen atoms for every 6 carbon atoms), guaiacol (1.5-to-6), and propyl guaiacol (1.5-to-9) were compared to the data (Fig. 6). This analysis reveals that >90% of the unique chemical formulas present in the CELF biocrudes fall within the range between syringol oligomers and propyl guaiacol oligomers. As the exact lignin structure is highly variable and remains incompletely characterized,[64] syringol and propyl guaiacol serve as characteristic monomers, wherein the space between these two extremes is representative of oligomers possessing one or more syringol or guaiacol units, among others, that lead to a nearly continuous range of molecular weights. The bracketing of the FT-MS data by syringol and propyl guaiacol compositions is therefore highly suggestive of the lignin subunit explanation of biocrude composition. Due to their thermal stability, the phenolic rings present in the lignin polymer do not undergo ring opening reactions, and only the linkages between monomers break during HTL. The resulting monomers than rearrange as they undergo repolymerization reactions with one another.

Qualitatively comparing the data to the slopes of the model oligomers provides additional insight. Based on the similar values of the slopes, the most representative oligomer in both samples was determined to be guaiacol. C-Bagasse biocrude contained a wider variety of monomers than C-Maple biocrude, as evidenced by the broader range of compositions present in its spectrum and consistent with H monomer units identified during GC-MS analysis of C-Bagasse biocrude. Comparing the model compounds projections to the data indicates that lignin biocrude was most likely to consist of oligomers possessing 2–5 monomers. Compared to the molecular weight of the CELF lignin feeds (Table 1), this finding is indicative of decreased biocrude molecular weight as a 5-monomer oligomer of syringol would result in a molecular weight of ~770 Da. By inference, the resultant char must consist of oligomers of more than 5 monomers and be the result of incomplete depolymerization and/or repolymerization of reactive intermediates.

Next, FT-ICR MS was used to probe the oligomeric nature of the biocrude based on oxygen heteroatom class abundance as a function of formula molecular weight (Fig. 7). The relative abundance of each oxygen heteroatom class (O_{1-12}) to the molecular mass of the identified formula was found to be consistent with the posited oligomeric nature of CELF lignin biocrude. For C-Bagasse, C-Poplar, and C-Maple, the highest relative abundance occurred between 500 and 550 Da, consistent with oligomers composed of ~4 monomers (guaiacol 4-mer = 496 Da; syringol 4-mer = 616 Da) – depending on side chains and linker groups – and bearing between 7 and 9 oxygen atoms. Fig. 7 is then broadly consistent with Fig. 6.

Interestingly, in addition to the peak molecular weights, C-Poplar and C-Maple contained clear evidence of a bi-modal distribution with a secondary peak between 350 and 400 Da dominated by compounds containing 5–7 oxygen atoms. C-Bagasse included a shoulder in this region that is not differentiated sufficiently to be termed a secondary peak and was absent from the FT-ICR MS analysis of K-Spruce (Fig. SI-10†), indicative of a syringol-dependent smaller oligomer (*i.e.* dimer or trimer). Accordingly, HTL of high S/G lignin feeds results in formation of an abundant sub-population of dimers and trimers that are less apparent in the biocrudes obtained from HTL of low S/G feeds.

Combining compositional analysis of the lignin feeds with biocrude yield, monomer yield, and FT-ICR-MS analysis of the biocrude heavy fraction provided the basis for CELF lignin selection for HTL conversion. When biocrude is the desired product, selecting feeds with high S/G ratio is recommended due to increased biocrude yield and decreased char yield compared to lower S/G CELF lignin. Practically, selecting high S/G lignin feeds implies selection of hardwood over agricultural

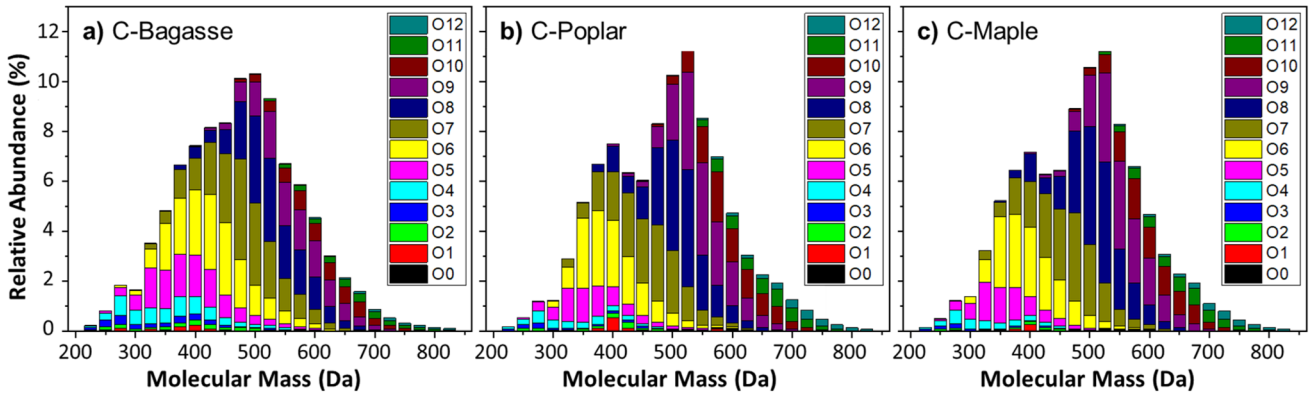

Fig. 7 Oxygen heteroatom class abundance as a function of molecular weight derived from the analysis of biocrude samples with 21 T (+) APPI FT-ICR MS for (a) C-Bagasse biocrude, (b) C-Poplar biocrude, and (c) C-Maple biocrude.

and especially softwood feeds. Low S/G CELF lignin may be best used for producing char, the yield of which can be maximized in the hydrothermal carbonization regime, as an intermediate to high value carbon materials in a biorefinery concept.[65] For maximizing monomer recovery, agricultural and grass feeds are preferred. HTL of agricultural feeds was found to yield monomers other than syringol and guaiacol, thereby boosting their total monomer yields.

One-step yields of monomers afforded by HTL are not competitive with techniques that utilize capping agents or flow-through reductive fractionation.[59,66–68] That stated, CELF pretreatment followed by HTL combined with mild hydrotreating will yield a mixture of cyclo-paraffinic and aromatic products with properties appropriate for gasoline or jet fuel, depending on the feedstock and the hydrotreating conditions.[15,69] Reaction conditions during hydrotreating can be tuned to maximize yields of individual, deoxygenated monomers or the corresponding oligomers consisting of up to 5 monomers. The results and analysis provided here guide selection of feedstocks for HTL and hydrotreating, which can be deployed as a hub-and-spoke configuration consisting of distributed HTL and centralized hydrotreating appropriate to maximize product value and minimize transportation costs.[70] Compared with capping methods, HTL followed by hydrotreating requires fewer auxiliary chemicals. Compared with flow-through reductive reactions, HTL followed by hydrotreating is less wasteful and more readily scaled.

Conclusions

Hydrothermal liquefaction of CELF-extracted lignin from five distinct biomass feedstocks representative of agricultural residues, softwood, and hardwood varieties elucidates effects of lignin chemical structure on HTL reactivity. Solid-state ^{13}C NMR, gel permeation chromatography, and elemental analysis were utilized to determine initial CELF lignin chemical characteristics, wherein a novel ^{13}C ssNMR composition analysis suitable for CELF lignin was developed.

Lignin S/G and degree of condensation were found to strongly correlate with biocrude yield and monomer composition. Char yield is negatively correlated with S/G ratio. Molecular analysis of the biocrude using FT-ICR-MS revealed the oligomeric content of the biocrude and provided insight into hydrotreating behavior. The results from these fundamental studies will inspire novel reactor and catalyst technologies to maximize lignin valorization potential.

Data availability

Most data are provided directly in the manuscript or ESI.† All other data are available upon request.

Conflicts of interest

There are no conflicts to declare.

Acknowledgements

The authors would like to acknowledge the Department of Energy Bioenergy Technology Office (DE-EE0008513) for funding this work. HOL was partially funded by the National Science Foundation GRF Program (#2038257). Funding for the solid-state NMR spectrometer utilized in this work was provided by the NSF MRI program (Award No. 1726346). A portion of this work was completed at the National High Magnetic Field Laboratory and supported by the National Science Foundation Division of Materials Research and Division of Chemistry through a Cooperative Agreement (DMR-1644779) and the state of Florida. All FT-ICR MS data is publicly available *via* Open Science Framework.

References

1 F. G. Calvo-Flores and J. A. Dobado, *ChemSusChem*, 2010, **3**, 1227–1235.
2 F. S. Chakar and A. J. Ragauskas, *Ind. Crops Prod.*, 2004, **20**, 131–141.
3 G. Gellerstedt, *Ind. Crops Prod.*, 2015, **77**, 845–854.
4 J. Gierer, *Wood Sci. Technol.*, 1980, **14**, 241–266.
5 J. Zakzeski, P. C. A. Bruijnincx, A. L. Jongerius and B. M. Weckhuysen, *Chem. Rev.*, 2010, **110**, 3552–3599.

6 T. Aro and P. Fatehi, *ChemSusChem*, 2017, **10**, 1861–1877.
7 A. Ekielski and P. K. Mishra, *Int. J. Mol. Sci.*, 2021, **22**(1), 63.
8 S. Sethupathy, G. Murillo Morales, L. Gao, H. Wang, B. Yang, J. Jiang, J. Sun and D. Zhu, *Bioresour. Technol.*, 2022, **347**, 126696.
9 L. Ana and P. Helena, in *Lignin*, ed. P. Matheus, IntechOpen, Rijeka, 2017, ch. 3, DOI: **10.5772/intechopen.71208**.
10 R. Katahira, T. J. Elder and G. T. Beckham, A Brief Introduction to Lignin Structure, in *Lignin Valorization: Emerging Approaches*, ed. G. T. Beckham, The Royal Society of Chemistry, 2018, pp. 1–20, DOI: **10.1039/9781788010351-00001**.
11 J. Ralph, C. Lapierre and W. Boerjan, *Curr. Opin. Biotechnol.*, 2019, **56**, 240–249.
12 E. T. Liakakou, B. J. Vreugdenhil, N. Cerone, F. Zimbardi, F. Pinto, R. André, P. Marques, R. Mata and F. Girio, *Fuel*, 2019, **251**, 580–592.
13 M. Sharifzadeh, M. Sadeqzadeh, M. Guo, T. N. Borhani, N. V. S. N. Murthy Konda, M. C. Garcia, L. Wang, J. Hallett and N. Shah, *Prog. Energy Combust. Sci.*, 2019, **71**, 1–80.
14 A. R. K. Gollakota, N. Kishore and S. Gu, *Renewable Sustainable Energy Rev.*, 2018, **81**, 1378–1392.
15 L. T. Funkenbusch, M. E. Mullins, L. Vamling, T. Belkhieri, N. Srettiwat, O. Winjobi, D. R. Shonnard and T. N. Rogers, *WIREs Energy and Environment*, 2019, **8**, e319.
16 M. Li, Y. Pu and A. J. Ragauskas, *Front. Chem.*, 2016, **4**, 45.
17 D. Min, C. Yang, R. Shi, H. Jameel, V. Chiang and H. Chang, *Biomass Bioenergy*, 2013, **58**, 52–57.
18 R. B. Santos, J. M. Lee, H. Jameel, H.-M. Chang and L. A. Lucia, *Bioresour. Technol.*, 2012, **110**, 232–238.
19 R. B. Santos, E. A. Capanema, M. Y. Balakshin, H.-M. Chang and H. Jameel, *BioResources*, 2011, **6**, 3623–3637.
20 S. Nakagame, R. P. Chandra, J. F. Kadla and J. N. Saddler, *Bioresour. Technol.*, 2011, **102**, 4507–4517.
21 Z. Yu, K.-S. Gwak, T. Treasure, H. Jameel, H.-M. Chang and S. Park, *ChemSusChem*, 2014, **7**, 1942–1950.
22 H. O. LeClerc, G. A. Tompsett, A. D. Paulsen, A. M. McKenna, S. F. Niles, C. M. Reddy, R. K. Nelson, F. Cheng, A. R. Teixeira and M. T. Timko, *iScience*, 2022, 104916, DOI: **10.1016/j.isci.2022.104916**.
23 C. Chen, D. Jin, X. Ouyang, L. Zhao, X. Qiu and F. Wang, *Fuel*, 2018, **223**, 366–372.
24 C. M. Cai, T. Zhang, R. Kumar and C. E. Wyman, *Green Chem.*, 2013, **15**, 3140–3145.
25 T. Y. Nguyen, C. M. Cai, R. Kumar and C. E. Wyman, *ChemSusChem*, 2015, **8**, 1716–1725.
26 M. D. Smith, B. Mostofian, X. Cheng, L. Petridis, C. M. Cai, C. E. Wyman and J. C. Smith, *Green Chem.*, 2016, **18**, 1268–1277.
27 A. Bhalla, C. M. Cai, F. Xu, S. K. Singh, N. Bansal, T. Phongpreecha, T. Dutta, C. E. Foster, R. Kumar, B. A. Simmons, S. Singh, C. E. Wyman, E. L. Hegg and D. B. Hodge, *Biotechnol. Biofuels*, 2019, **12**, 213.
28 B. C. Klein, B. Scheidemantle, R. J. Hanes, A. W. Bartling, N. J. Grundl, R. J. Clark, M. J. Biddy, L. Tao, C. T. Trinh, A. M. Guss, C. E. Wyman, A. J. Ragauskas, E. G. Webb, B. H. Davison and C. M. Cai, *Energy Environ. Sci.*, 2024, **17**, 1202–1215.
29 X. Meng, A. Parikh, B. Seemala, R. Kumar, Y. Pu, P. Christopher, C. E. Wyman, C. M. Cai and A. J. Ragauskas, *ACS Sustainable Chem. Eng.*, 2018, **6**, 8711–8718.
30 S. V. Pingali, M. D. Smith, S.-H. Liu, T. B. Rawal, Y. Pu, R. Shah, B. R. Evans, V. S. Urban, B. H. Davison, C. M. Cai, A. J. Ragauskas, H. M. O'Neill, J. C. Smith and L. Petridis, *Proc. Natl. Acad. Sci. U.S.A.*, 2020, **117**, 16776–16781.
31 X. Meng, S. Zhang, B. Scheidemantle, Y.-y. Wang, Y. Pu, C. E. Wyman, C. M. Cai and A. J. Ragauskas, *Ind. Crops Prod.*, 2022, **178**, 114579.
32 Y.-Y. Wang, B. Scheidemantle, C. E. Wyman, C. M. Cai and A. J. Ragauskas, *Biomacromolecules*, 2021, **22**, 2129–2136.
33 Z.-M. Zhao, X. Meng, B. Scheidemantle, Y. Pu, Z.-H. Liu, B.-Z. Li, C. E. Wyman, C. M. Cai and A. J. Ragauskas, *Bioresour. Technol.*, 2022, **347**, 126367.
34 N. Kothari, E. K. Holwerda, C. M. Cai, R. Kumar and C. E. Wyman, *Biotechnol. Biofuels*, 2018, **11**, 219.
35 V. A. Thomas, B. S. Donohoe, M. Li, Y. Pu, A. J. Ragauskas, R. Kumar, T. Y. Nguyen, C. M. Cai and C. E. Wyman, *Biotechnol. Biofuels*, 2017, **10**, 252.
36 H. O. LeClerc, R. Atwi, S. F. Niles, A. McKenna, M. T. Timko, R. H. West and A. R. Teixeira, *Green Chem.*, 2022, **24**, 5125–5141.
37 J. D. Mao and K. Schmidt-Rohr, *Environ. Sci. Technol.*, 2004, **38**, 2680–2684.
38 C. L. Hendrickson, J. P. Quinn, N. K. Kaiser, D. F. Smith, G. T. Blakney, T. Chen, A. G. Marshall, C. R. Weisbrod and S. C. Beu, *J. Am. Soc. Mass Spectrom.*, 2015, **26**, 1626–1632.
39 D. F. Smith, D. C. Podgorski, R. P. Rodgers, G. T. Blakney and C. L. Hendrickson, *Anal. Chem.*, 2018, **90**, 2041–2047.
40 H. O. LeClerc, J. R. Page, G. A. Tompsett, S. F. Niles, A. M. McKenna, J. A. Valla, M. T. Timko and A. R. Teixeira, *ACS Sustainable Chem. Eng.*, 2023, **11**(6), 2427–2439.
41 C.-L. Chen and D. Robert, in *Methods in Enzymology*, Academic Press, 1988, vol. 161, pp. 137–174.
42 K. M. Holtman, H.-M. Chang, H. Jameel and J. F. Kadla, *J. Wood Chem. Technol.*, 2006, **26**, 21–34.
43 Z. Xia, L. G. Akim and D. S. Argyropoulos, *J. Agric. Food Chem.*, 2001, **49**, 3573–3578.
44 R. L. Johnson and K. Schmidt-Rohr, *J. Magn. Reson.*, 2014, **239**, 44–49.
45 J. Mao, K. M. Holtman, J. T. Scott, J. F. Kadla and K. Schmidt-Rohr, *J. Agric. Food Chem.*, 2006, **54**, 9677–9686.
46 G. Gellerstedt and E.-L. Lindfors, *Holzforschung*, 1984, **38**, 151–158.
47 A. T. Martínez, G. Almendros, F. J. González-Vila and R. Fründ, *Solid State Nucl. Magn. Reson.*, 1999, **15**, 41–48.
48 S. J. Opella and M. H. Frey, *J. Am. Chem. Soc.*, 1979, **101**, 5854–5856.
49 Z. Zheng and K. Schmidt-Rohr, *Solid State Nucl. Magn. Reson.*, 2024, **133**, 101947.
50 W. F. Manders, *Holzforschung*, 1987, **41**, 13–18.
51 B. M. Upton and A. M. Kasko, *Chem. Rev.*, 2016, **116**, 2275–2306.

52 S. K. Bose, R. C. Francis, M. Govender, T. Bush and A. Spark, *Bioresour. Technol.*, 2009, **100**, 1628–1633.
53 R. B. Santos, E. A. Capanema, M. Y. Balakshin, H.-m. Chang and H. Jameel, *J. Agric. Food Chem.*, 2012, **60**, 4923–4930.
54 E. M. Anderson, M. L. Stone, R. Katahira, M. Reed, W. Muchero, K. J. Ramirez, G. T. Beckham and Y. Román-Leshkov, *Nat. Commun.*, 2019, **10**, 2033.
55 F. J. F. Lopes, F. O. Silvério, D. C. F. Baffa, M. E. Loureiro and M. H. P. Barbosa, *Journal of Water Chemistry and Technology*, 2011, **31**, 309–323.
56 K. Hodgson-Kratky, V. Perlo, A. Furtado, H. Choudhary, J. M. Gladden, B. A. Simmons, F. Botha and R. J. Henry, *Plant Mol. Biol.*, 2021, **106**, 173–192.
57 G. Moxley, A. R. Gaspar, D. Higgins and H. Xu, *J. Ind. Microbiol. Biotechnol.*, 2012, **39**, 1289–1299.
58 A.-M. Saariaho, A.-S. Jääskeläinen, M. Nuopponen and T. Vuorinen, *Appl. Spectrosc.*, 2003, **57**, 58–66.
59 X. Huang, T. I. Korányi, M. D. Boot and E. J. M. Hensen, *Green Chem.*, 2015, **17**, 4941–4950.
60 K. H. Kim and C. S. Kim, *Frontiers in Energy Research*, 2018, **6**, 92.
61 F. Cheng, Z. Cui, L. Chen, J. Jarvis, N. Paz, T. Schaub, N. Nirmalakhandan and C. E. Brewer, *Appl. Energy*, 2017, **206**, 278–292.
62 J. M. Jarvis, J. M. Billing, Y. E. Corilo, A. J. Schmidt, R. T. Hallen and T. M. Schaub, *Fuel*, 2018, **216**, 341–348.
63 N. Sudasinghe, B. Dungan, P. Lammers, K. Albrecht, D. Elliott, R. Hallen and T. Schaub, *Fuel*, 2014, **119**, 47–56.
64 Y. Cao, S. S. Chen, S. Zhang, Y. S. Ok, B. M. Matsagar, K. C. W. Wu and D. C. W. Tsang, *Bioresour. Technol.*, 2019, **291**, 121878.
65 R. K. Mishra, V. kumar, P. Kumar and K. Mohanty, *Fuel*, 2022, **316**, 123377.
66 T. Belkheiri, S.-I. Andersson, C. Mattsson, L. Olausson, H. Theliander and L. Vamling, *Energy Fuels*, 2018, **32**, 5923–5932.
67 F. Hernández-Ramos, J. Fernández-Rodríguez, M. G. Alriols, J. Labidi and X. Erdocia, *Fuel*, 2020, **280**, 118524.
68 T. Renders, G. Van den Bossche, T. Vangeel, K. Van Aelst and B. Sels, *Curr. Opin. Biotechnol.*, 2019, **56**, 193–201.
69 J. Yu, P. Biller, A. Mamahkel, M. Klemmer, J. Becker, M. Glasius and B. B. Iversen, *Sustainable Energy Fuels*, 2017, **1**, 832–841.
70 M. Shahabuddin, E. Italiani, A. R. Teixeira, N. Kazantzis and M. T. Timko, *ACS Sustainable Chem. Eng.*, 2023, **11**, 733–743.